Differential Thermal Analysis of Metal–Ammonia Solutions

K. MEHTA AND N. MAMMANO

Department of Chemistry, State University of New York, College of Arts and Science, Plattsburgh, New York 12901

Differential thermal analysis measurements have established eutectic and anomaly transition temperatures for Eu–NH$_3$ and Yb–NH$_3$ solutions. The dependence of eutectic and anomaly transition heats on composition for Sr–NH$_3$ solutions provide strong evidence for solid solution formation. The anomaly is interpreted as a peritectoid reaction; solid solution → solid hexammine + solid NH$_3$.

Introduction

Metal–ammonia systems have been the focus of an enormous number of studies for over a century (*1–3*). It is only within the past decade, however, that the solid compounds formed from these systems have become objects of any intensive investigation. The metals which are known to combine with NH$_3$ to form "ammines" are Li, Ca, Sr, Ba, Eu, and Yb. The properties of lithium tetrammine, Li(NH$_3$)$_4$, have been somewhat more thoroughly investigated, primarily because of its rather unique phase behavior and its interesting solid-state characteristics. The alkaline earth metals, Ca, Sr, and Ba, and the lanthanide metals, Eu and Yb, form hexammines of approximate stoichiometry M(NH$_3$)$_6$; these golden, metallic hexammines have not been as thoroughly studied as Li(NH$_3$)$_4$, and information on them is relatively meager. A review of their properties may be found in Ref. *3*. Recently some analyses of the thermodynamic stability of the hexammines based on vapor pressure data (*4a–d*), as well as a Mössbauer study (*5*) of Eu–NH$_3$ have become available.

One particularly extensive area of investigation in metal–ammonia systems has been their phase behavior. Metal–ammonia compounds are typically prepared in liquid metal–ammonia solutions, and at relatively accessible temperatures and pressures the several heterogenous equilibria in the binary system may be conveniently studied. Although the M–NH$_3$ system is a relatively simple binary type, the information relating to its phase behavior is sketchy and ambiguous. The temperature-composition diagram for lithium–NH$_3$ is exceedingly unusual (*6*); virtually all of the data on the solid existing at low temperature is consistent with the formation of a tetrammine, Li(NH$_3$)$_4$ (*7*), yet this solid compound does not appear to exist in equilibrium with the liquid melt [absence of congruent or incongruent melting (*8*)]. The alkaline earth/NH$_3$ systems show wide ranges in stoichiometry (*9*) [attributed to vacancies and/or interstitial ammonia (*10*)]. A number of anomalies (*11, 12*) have been detected by thermal, magnetic, and conductivity studies; the nature of these anomalies and their significance in terms of the phase behavior and solid-state characterization of the metal ammines is a matter of continuing speculation.

In this work we present further investigations of the alkaline-earth and lanthanide metal–ammonia systems. A differential thermal analysis technique has been employed to confirm previously reported eutectic and anomaly temperatures for the NH$_3$-rich portion of the phase diagram for ammonia solutions of Ca, Sr, and Ba and to determine these points for Eu– and Yb–ammonia systems. Moreover, we have systematically investigated the variation of the transition heats with composition for Sr–NH$_3$ over a range of 2–13 % metal.

Experimental

A differential thermal analysis (DTA) apparatus was constructed similar to one described by Sienko (*13*). The sample and reference cells,
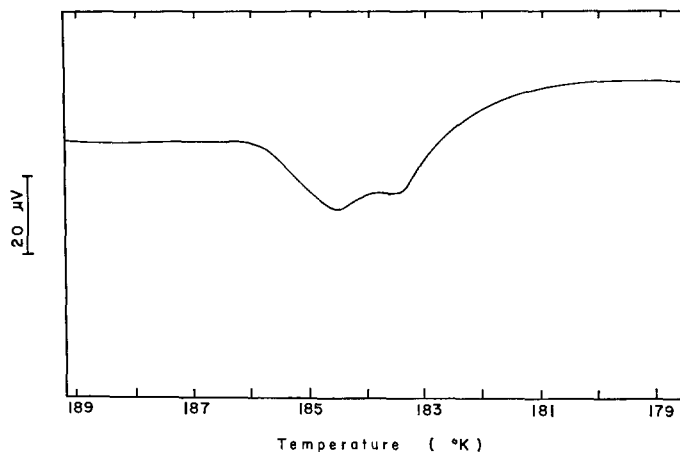
FIG. 1. Cooling DTA thermogram for a 4% Ca–NH₃ solution.

constructed from 9-mm Pyrex tubing, were contained in a "block" consisting of a 4 in. × 1½ in. copper cylinder filled with aluminum powder; this powder was also placed in the reference cell as the thermal reference material. The Pyrex tubes were reproducibly located within the block with metal spacing discs. Copper/constantan thermocouple junctions were imbedded in a well at the bottom of each cell with epoxy cement, and the difference EMF was amplified and recorded with a L & N AZAR recorder. No additional amplification stage between thermocouples and recorder was necessary; with sample sizes employed (50–300 mg), the smallest transition detected produced a maximum EMF of approximately 10 μV (0.3°C). Heating was effected by a noninductive coil of constantan wound around the copper cylinder. Transition temperatures were measured with a third Cu/constantan thermocouple placed adjacent to the sample cell; a White potentionmeter was used to measure this EMF.

The copper cylinder was suspended in a small Dewar flask, and slow cooling to the initial temperature for a run was carried out by placing a small quantity of liquid N_2 in the bottom of the Dewar several inches below the bottom of the cell. When the desired temperature was attained, the liquid N_2 was poured off, the Dewar replaced, and a warming cycle initiated. In general, temperatures and transition heats were determined by warming (the warming rate was 1.2°C/min), with the exception of the run to determine the anomaly and eutectic temperature for Ca–NH₃. Because of the closeness of the two

transitions in this latter system, the warming cycle was not unambiguous in resolving these two temperatures. A cooling thermogram (cooling rate, 0.3°C/min), however, clearly showed the presence of the anomaly just below the eutectic (Fig. 1). Further confirmation was furnished by a simple cooling curve, in which the sample temperature was monitored directly as a function of time by connecting the third thermocouple, adjacent to the sample cell, directly to the recorder. The breaks in the curve are clearly discernible in Fig. 2.

Samples were prepared *in situ* at 208°K by condensing known amounts of NH₃ (Matheson, 99.99%) on a weighed sample of metal in the DTA sample cell (the metal previously added in a glove bag under N_2). The metals used were obtained from Alfa Inorganics and had the following purities: Ca, 99.5%; Sr, 99+%; Ba, 99.5%; Eu, 99.9%; Yb, 99.5%. The quantity of NH₃ was determined from the ideal gas equation by measuring the pressure and temperature of a calibrated volume on a vacuum line. Reaction of metal with ammonia was observed to be quite slow at 208°K; completion of the solution reaction, as determined by the reproducibility of the transition heats measured, was often attained only after 20–24 hr at 208°K. The pressure was periodically monitored during the measurements and no decomposition was observed.

The composition of the NH₃-rich Sr–NH₃ eutectic has been reported by Birch and MacDonald (*11*) as 7 mole% Sr. In this work, concentration was varied by the addition or removal of known quantities of NH₃; metal
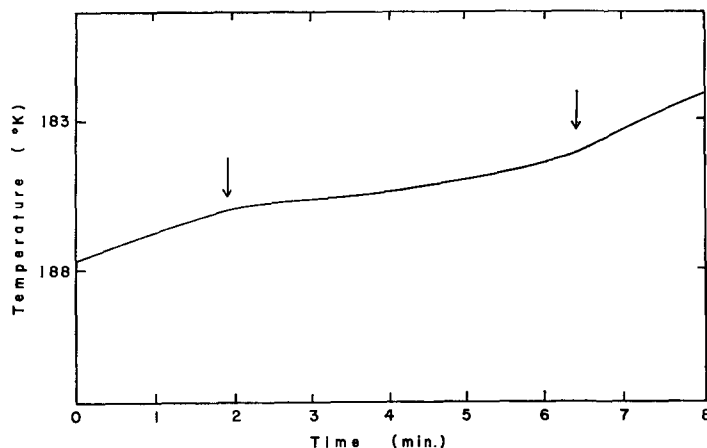
14

FIG. 2. Cooling curve for the same 4% Ca-NH₃ solution, showing the "breaks" at the 186°K eutectic and the 184°K anomaly. This curve was obtained by directly monitoring the sample temperature with time.

composition was decreased by adding NH_3 to solutions more dilute than 7% metal, and increased by removing NH_3 from solutions more concentrated than 7%. The latter step was necessary because the steep solubility curve for $Sr(NH_3)_6$ (by analogy with the Ca–NH_3 diagram) (2) required that solutions be prepared NH_3-rich in order to have a homogeneous liquid solution of known composition initially. Sr–NH_3 was selected as the system to determine transition heats as a function of composition since it was the most stable.

Transition heats were calculated by measuring curve areas with a planimeter, the cell having previously been calibrated under the same experimental conditions by determining the area under the melting thermogram of a known weight of mercury (heat of melting = 2.735 cal/g).

Results

Birch and MacDonald (11) have reported transition temperatures for the alkaline earth–NH_3 systems: eutectic temperatures, Ca, 186°K; Sr, 184°K; Ba, 184°K; anomaly temperatures, Ca, 184°K; Sr, 175°K; Ba, 164°K. We have confirmed these results and have also determined the corresponding temperatures for Eu–NH_3 (eutectic, 184°K; anomaly, 176°K) and Yb–NH_3 (eutectic, 184°K; anomaly, 177°K). It is interesting to note that, in each case, the eutectic temperatures occur at 184°K, with the exception of Ca–NH_3. The suspicion arose that the temperature attributed to the anomaly at 184°K may indeed be the eutectic, with perhaps the anomaly

TABLE I

TRANSITION HEAT DATA FOR STRONTIUM–AMMONIA SYSTEMS

Composition (%Sr)	Heat of transition[d] (cal/mole of Sr)	
	Eutectic (184°K)	Anomaly (175°K)
2.5[a]	702	181
3.0[a]	833	239
4.0[a]	1021	304
5.5[a]	1818	435
5.5[b]	1645	425
6.5[b]	3087	497
7.0[c]	3843	623
9.0[c]	2700	560
13.0[c]	0	0

[a,b,c] Data obtained from different samples.

[d] Within ±5%. We believe the uncertainty is largely due to variations in sample "packing" in the DTA sample cell.

occurring at the higher temperature 186°K. In the absence of a mechanical test to establish whether the system actually freezes completely at 186°K, we took the relative areas under the eutectic and anomaly transition curves for identification since, in the other metal–NH_3 systems, the eutectic heat was 4–5 times larger than the anomaly transition heat. The cooling thermogram for a 4% sample of Ca–NH_3 is shown in Fig. 1, and, clearly, the first transition at 184°K, which we take to be the eutectic, has a larger area, the anomaly appearing as a shoulder at 184°K.
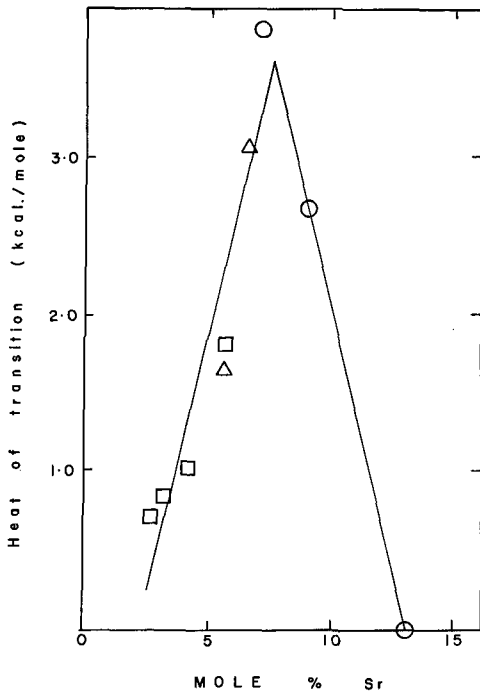
FIG. 3. Eutectic transition heat versus composition for Sr–NH₃ solutions; the circles, squares, and triangles refer to data taken on different samples.
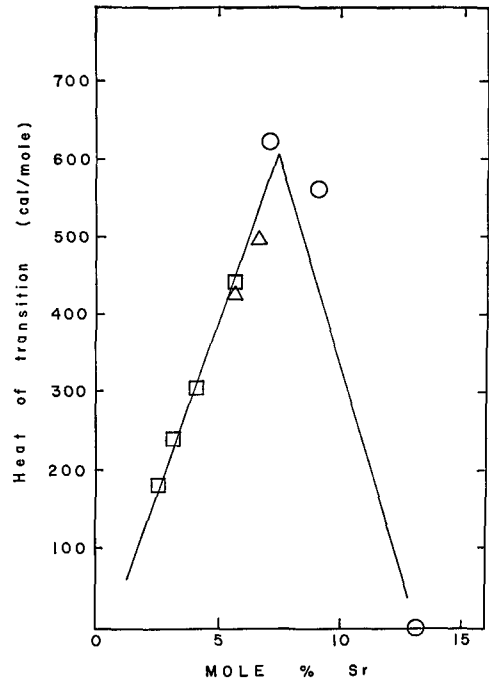
FIG. 4. Anomaly transition heat versus composition for Sr–NH₃ solutions.

The composition data for Sr–NH₃ is given in Table I and is presented in Fig. 3 for the eutectic and in Fig. 4 for the anomaly. Since the data were obtained at different times on differing quantities of solution, the coordinate is given as cal/mole of Sr by employing the mercury calibration. A

typical thermogram for Sr–NH₃ is shown in Fig. 5 (11); the peak close to 189°K represents the base of the liquid–liquid separation "dome" which is an invariant point; our data indicate that the right side of this miscibility gap (concentrated liquid) intersects (point M, Fig. 6) the
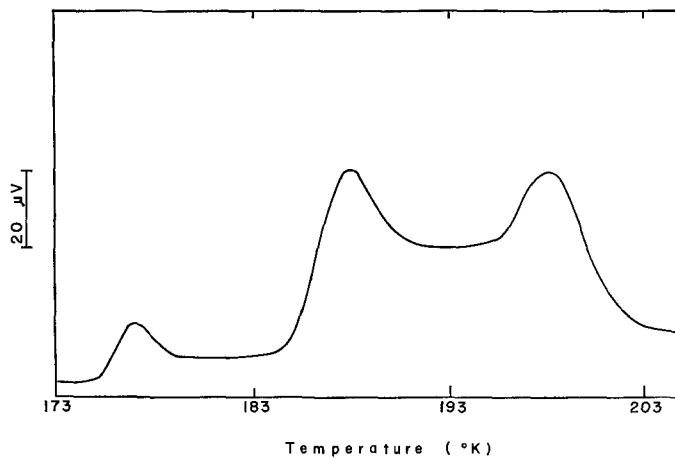

FIG. 5. Typical warming DTA thermogram for Sr–NH₃. The peaks represent anomaly, eutectic, and liquid–liquid separation points, respectively, with increasing temperature, and are inverted, of course, compared to those of Fig. 1, since the transitions are exothermic for a cooling cycle and endothermic for a warming cycle.
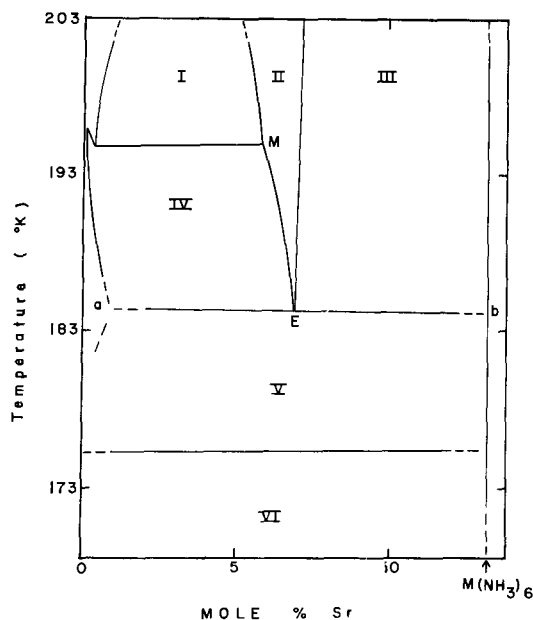
FIG. 6. Suggested phase diagram for part of the NH_3-rich portion of the Sr-NH_3 phase diagram, showing solid solution formation. Point M, composition of concentrated liquid at approximately 195°K; E, eutectic; a, approximate composition of solid solution at 184°K; b, $M(NH_3)_6$. The Roman numerals correspond to areas where the following phase(s) exist(s) in equilibrium: 1, 2 liquid solutions; II, 1 liquid solution; III, $Sr(NH_3)_6(s)$ + liquid; IV, solid solution + liquid; V, solid solution + $Sr(NH_3)_6$; VI, $NH_3(s)$ + $Sr(NH_3)_6$.

NH_3 freezing point line at 5.5% Sr. The intersection with the left-hand side of the miscibility gap (dilute liquid) was not detectable because of the compressed NH_3 solubility curve at very high dilution (2). Our work also confirms Birch and MacDonald's NH_3 solubility curve (line ME, Fig. 6). No other transitions were observed for any metal solution down to 77°K.

Discussion

Phase diagrams constructed for alkaline earth–NH_3 systems have taken the NH_3-rich eutectic to represent the intersection of the freezing point curves of $M(NH_3)_6$ and NH_3 in the liquid solution (2); the eutectic solid would then consist of a finely divided two-phase mixture of solid $M(NH_3)_6$ and solid NH_3. [We are taking the compound to be stoichiometric $Sr(NH_3)_6$ here and in the arguments to follow, although vapor pressure (9) and X ray data (10) clearly indicate that metal lattice vacancies and/or interstitial

ammonia may lead to considerable variation in the NH_3/metal ratio.] For Sr-NH_3, the eutectic melting reaction at 184°K would therefore be represented by

$Sr(NH_3)_6(s) + NH_3(s) \rightarrow$ Sat'd Sol'n (7% Sr).
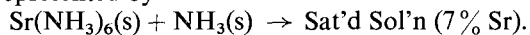
The data in Fig. 3 are not consistent with this picture, but indicate that it is not pure solid ammonia which is precipitating, but rather a solid solution of $Sr(NH_3)_6$ in NH_3 (14). The figure shows the eutectic heat of transition decreasing as the solution is diluted with NH_3; this is primary evidence for solid solution formation since, if NH_3 existed as the pure solid in this system, the excess NH_3 added on dilution would simply freeze at higher temperatures along the NH_3 freezing-point line, leaving the amount of eutectic material, and therefore the eutectic transition heat, unchanged. The decrease with added NH_3 indicates that the quantity of eutectic solid is also decreasing, and this is consistent with the added NH_3 being precipitated as a solid solution containing Sr [as $Sr(NH_3)_6$]. The Sr which must be dissolved in the added NH_3 can only be obtained at the expense of the $Sr(NH_3)_6$ in the eutectic solid, since this is the only source of Sr for the NH_3-rich system to the left of the 7% eutectic. Since the relative amounts of the phases in the eutectic are fixed (given by the tie lines Ea and Eb in Fig. 6), the total amount of eutectic material must also decrease, if the quantity of $Sr(NH_3)_6$ decreases. In Fig. 6 the eutectic heat would be a maximum at E and vanish at a and b.

The composition data for the 175°K anomaly, shown in Fig. 4, yield the same dependence as the eutectic transition heat; a maximum close to 7%, decreasing with apparent linearity to either side. The results clearly indicate that the anomaly is associated in some way with the material precipitating *at the eutectic*, i.e., the finely divided two-phase mixture of $Sr(NH_3)_6$ and Sr-NH_3 solid solution, which precipitates isothermally at 184°K. The composition dependence observed in this work, together with earlier data on conductivity (11) and powder X ray diffraction (15), [the former indicated increased conductivity on cooling through 184°K, the latter indicated that there is no change in the bcc structure of $M(NH_3)_6$] strongly suggest that the anomaly may be associated with an "interaction" between compound $Sr(NH_3)_6$ and solid solution. We believe that this interaction is the coagulation of solvated $Sr(NH_3)_6$ units in the solid solution, into metallic $Sr(NH_3)_6$, with attendant electron de-

localization and band formation. Thus we suggest that at 175°K, solvated $Sr(NH_3)_6$ precipitates from the solid solution phase in the finely divided eutectic, and augments the existing $Sr(NH_3)_6$ phase there. The abstraction of $Sr(NH_3)_6$ units from the solid ammonia solvent into the metallic $Sr(NH_3)_6$ phase would only be possible in the finely divided eutectic mixture according to Figs. 3 and 4, which show that the amount of material reacting or transforming at 175°K varies in the same way as the amount of material at 184°K. Indeed, we are suggesting that it is the same material involved at both transitions; it is the finely divided nature of the eutectic phases which makes the (peritectoid) reaction at the anomaly possible.

The "blue solid" which has been cited (15) on evaporation of ammonia from solutions of the alkaline earth metals may be a solid solution of Sr in NH_3. Sienko has made the interesting suggestion that this blue solid is a "strongly ammonia-rich hexammine and that the blue-to-bronze, nonmetal-to-metal transition observed in the liquid solution, is also seen in the solid state." The model proposed in this work is consistent with Sienko's suggestion if the anomaly is viewed as the base of a solid–solid miscibility gap, where solid NH_3 is precipitated from the (dilute) solid solution to yield the (concentrated) solid solution, i.e., $Sr(NH_3)_6$. The miscibility gap would, of course, be interrupted by eutectic melting, only 9 degrees higher in the Sr–NH_3 case, and an upper consolute temperature would not be attainable.

The trend observed in the anomaly transition temperatures for the different metal systems is also consistent with coagulation of $M(NH_3)_6$ units and electron delocalization to form a metal. One would predict, as a first approximation, that the tendency for electron delocalization and band formation would be dependent on the ionization potentials and atomic radii of the metals involved. With the exception of Yb/NH_3, the data shown in Table II support this view. The table gives r_a, atomic radius, E (sum of first and second ionization potentials) and T_a (anomaly temperature) for the metals of interest. For Ca, Eu, Sr, and Ba, the trend in T_a with r_a or E is as expected; the lower the transition temperature, the lower the barrier for delocalization and band formation, which in turn would be facilitated by a low ionization potential sum and/or large radius. The exceptional behavior of Yb is not novel; Senozan (4d) has determined the gaseous

TABLE II

ATOMIC RADIUS IONIZATION POTENTIAL AND ANOMALY TRANSITION TEMPERATURE

Metal	r_a (Å)[a]	E (eV/mole)	T_a (°K)
Yb	1.94	18.35[b,c]	177
Ca	1.97	17.91[a]	184
Eu	1.99	16.04[d,e]	176
Sr	2.15	16.64[a]	175
Ba	2.18	15.14[a]	164

[a] "Handbook of Chemistry and Physics," 51st edit., Chemical Rubber Publishing Co., Cleveland, Ohio, 1970–1971.
[b] A. C. Parr and M. C. Ingram, *J. Chem. Phys.* **52**, 4916 (1970).
[c] A. C. Parr and F. A. Elder, *J. Chem. Phys.* **49**, 26 (1968).
[d] J. Reader and J. Sugar, *J. Opt. Soc. Amer.* **56**, 1189 (1966).
[e] J. Sugar and J. Reader, *J. Opt. Soc. Amer.* **55**, 1286 (1965).

ammoniation energies of the divalent ions and observed that "Yb^{2+} falls slightly out of the pattern of alkaline earth ions." The anomalous result was attributed to an underestimation of ionic radius in that work; taking the ionic radius to be "only 0.05 Å greater" would allow Yb^{2+} to fall in line with the other metal cations. A similar "correction" of 0.04 Å in the atomic radius in this work places Yb/NH_3 in sequence with respect to its anomaly transition temperature, although the large ionization potential for Yb suggests that the model is oversimplified and that, at least with respect to this metal, there are other energetic factors contributing to its position in the sequence.

In this respect, it is interesting to note further the virtual lack of a trend in the eutectic temperatures for the metal–NH_3 systems studied. Since the eutectic temperature represents the intersection of M/NH_3(s) and $M(NH_3)_6$(s), freezing point curves a similar dependence of temperature with metal system would be expected. The identity of eutectic temperatures suggests that the solubilities of the solids and their temperature dependencies are independent of the particular metal and probably overridingly dependent on the constituent common to all the systems, the solvated electron. In this regard, the resemblance between these saturated solutions and the blue dilute solutions, whose properties are dominated by the solvated electron, is striking.

The picture presented above relating to the

nature of the eutectic and the anomaly may also prevail in the Li–NH$_3$ system; in that case, an 82°K "anomaly" occurs below an 89°K "eutectic". Transition heat data for each of these two transitions do not show the same dependence with composition as do the alkaline earth– and lanthanide–NH$_3$ systems; the transition heats are independent of NH$_3$ for NH$_3$-rich solutions, apparently ruling out solid solution formation (8). The phase data point to the absence of a maximum in the temperature-composition diagram and to the presence of a simple binary eutectic of Li(s) and NH$_3$(s), but the unusual properties observed for the solid (high heat capacity (8), high metallic conductivity (6), bronze color) strongly suggest that it contains metallic Li(NH$_3$)$_4$. In accord with the model we have presented above for the Sr/NH$_3$ "eutectic" as a finely divided, two-phase mixture containing a marginally metallic solid solution, the Li–NH$_3$ solid existing between 82°K and 89°K may be similarly interpreted. We suggest that the 89°K transition is a true eutectic equilibrium, where a 20% saturated lithium–NH$_3$ solution yields a finely divided two-phase mixture of Li(s) and NH$_3$(s) on cooling. The relatively high Li content of this solid, compared to the solid solution phase of the Sr/NH$_3$ eutectic, may account for the observed metallic behavior between 82° and 89°K. Indeed, because of the uniquely sub-divided nature of the eutectic, electron delocalization among lithium metal "islands" in a sea of NH$_3$, as a separate thermodynamic phase, may already exist. As the temperature is lowered to 82°K, the peritectoid reaction, Li(s) + 4NH$_3$(s) → Li(NH$_3$)$_4$(s), consistent with the observed properties at lower temperatures, occurs. The 82–89°K solid is not a solid solution, but a two-phase eutectic, because it does not meet the primary requirement of a solid solution, variable composition. Its composition is fixed at 20% lithium, by virtue of the fact that Li(s) and NH$_3$(s) solubility curves intersect at 89°K at this composition and, therefore, fix the composition of the finely divided eutectic at 20% Li.

The characterization of the 82–89°K region as a binary eutectic, of solid lithium and solid ammonia, albeit with unusual properties, should be possible by an X ray study, since the X ray patterns of both phases should be distinguishable. The earlier X ray investigation of the 20% Li–NH$_3$ system by powder methods was done at 77°K, and the identity of the 82–89°K phase could only be inferred (7). If another X ray study

could be performed, coupled with *precise* temperature control between 82–89°K (by perhaps using boiling oxygen or boiling argon as the refrigerant, or even quenching the 82–89°K phase to 4°K where liquid helium could be conveniently employed), the unambiguous identification of the intriguing 82–89°K phase should be attained.

Acknowledgment

References

1. W. L. JOLLY, *Progr. Inorg. Chem.* **1**, 235 (1959).
2. G. LEPOUTRE AND M. J. SIENKO, Eds., "Metal-Ammonia Solutions" (Colloque Weyl I). W. A. Benjamin, New York, 1964. Specifically, see the articles by M. J. Sienko, p. 23, and R. Catterall, p. 41, for discussions of phase diagrams in metal–ammonia systems.
3. J. J. LAGOWSKI AND M. J. SIENKO, Eds., "Metal-Ammonia Solutions" (Colloque Weyl II). Butterworths, London, 1970. Specifically, see the article by N. Mammano, p. 367, for a discussion of solid metal–ammonia compounds.
4. A. S. DICKMAN, N. M. SENOZAN, AND R. L. HUNT, *J. Chem. Phys.* **52**, 2657 (1970).
   b. G. MAST AND N. M. SENOZAN, *J. Chem. Phys.* **53**, 1296 (1970).
   c. G. PLUMMER AND N. M. SENOZAN, *J. Chem. Phys.* **55**, 4062 (1971).
   d. R. H. FRISBEE AND N. M. SENOZAN, *J. Chem. Phys.* **57**, 1248 (1972).
5. J. P. BROWN, R. L. COHEN, AND K. W. WEST, *Chem. Phys. Letters*, (1973).
6. J. A. MORGAN, R. L. SCHROEDER, AND J. C. THOMPSON, *J. Chem. Phys.* **43**, 4494 (1965).
7. N. MAMMANO AND M. J. SIENKO, *J. Amer. Chem. Soc.* **90**, 6322 (1968).
8. N. MAMMANO AND L. V. COULTER, *J. Chem. Phys.* **50**, 393 (1969).
9. P. R. MARSHALL AND H. J. HUNT, *J. Phys. Chem.* **60**, 732 (1956).
10. F. W. CAGLE AND H. J. HOLLAND, presented at the 145th National Meeting of the American Chemical Society, New York, September 1963.
11. A. J. BIRCH AND D. K. C. MACDONALD, *Trans. Faraday Soc.* **44**, 735 (1948).
12. H. OESTERREICHER, N. MAMMANO, AND M. J. SIENKO, *J. Solid State Chem.* **1**, 10 (1969).
13. M. J. SIENKO, private communication.
14. J. E. RICCI, "The Phase Rule and Heterogeneous Equilibrium," pp. 190–194. Dover, New York, 1966.
15. N. MAMMANO AND M. J. SIENKO, *J. Solid State Chem.* **1**, 534 (1970).